

Measurement of Directionally Resolved Radar Cross Section of Human Body for 140 and 220 GHz Bands

Naveed A. Abbasi, Andreas F. Molisch
Wireless Devices and Systems Group (WiDeS)
Viterbi School of Engineering
University of Southern California
{nabbasi, molisch}@usc.edu

Jianzhong Charlie Zhang
Samsung Electronics
Richardson, TX USA
jianzhong.z@samsung.com

Abstract—To explore the eventual deployment of communication systems in Terahertz (THz) band (0.1-10 THz) frequencies, extensive measurements of various aspects of the channels are essential. Humans form an integral part of any communication environment, therefore, it is of interest to explore the impact of a human body on the propagation characteristics in any given channel. This is particularly relevant because at higher frequencies, such as those in the THz band, human bodies are significantly larger than a wavelength and can thus constitute effective scatterers. Motivated by this, we conducted measurements of the radar cross section for the human body in the 140 and 220 GHz bands and show how the reflectivity of the human body varies as a function of both the angle of incidence and the angle of observation. Our results show an average scattering cross sections on the order of -15 dBsm; with variations as a function of the angle of incidence of less than +/- 5 dBsm.

Index Terms—Terahertz (THz) band, radar cross section, human body.

I. INTRODUCTION

The demands for higher data rates for applications such as high-resolution videos and virtual reality are increasing constantly. In order for the technology to satisfy consumer needs, next-generation wireless networks need to realize data rates reaching terabits per second (Tbps) while also supporting higher connection density [1], [2]. Hence, researchers around the world are exploring the Terahertz (THz) Band (0.1 - 10 THz) [3]–[8] where very large swaths of spectrum are either available now, or are expected to become available in the future. In this regard, recent interest by Federal Communication Commission (FCC) is noticeable where sub-bands in the THz band between 140-220 GHz were earmarked for experimental licenses to encourage research [9].¹

The small wavelength of THz signals provides the potential of building antenna arrays with a large number of elements (> 1000) that can be fit into a reasonable form factor [10]. Yet, despite these opportunities, THz communications faces a number of challenges. Atmospheric characteristics play a

This work was supported by the Semiconductor Research Corporation (SRC) under the ComSenTer program.

¹While the 140-220 GHz band is strictly speaking “high mm-wave band”, we will follow here the widely used nomenclature of calling it “THz”.

major role in communication links operating above 100 GHz, since molecular absorption may lead to high signal losses. Moreover, higher frequencies, being highly directional, are more easily blocked by any obstacles on their path. Finally, since the ultimate application of a communication scheme is highly dependent on the scenario for its use, it is pertinent to have knowledge of key components of each relevant scenario, but measurements for many of such effects are missing.

Up to now, most of the interest for THz communications has concentrated on short range indoor scenarios, such as information kiosks in the 300 GHz band [11]–[14], however, some relatively long distance outdoor measurements have also been conducted [15]. However, these measurements generally do not include the presence of human bodies in the environment - and as a matter of fact, the measurement setup design explicitly excludes them. Yet almost all practical deployments will have humans as part of the propagation environment, and their effect on the propagation will be much more significant than at lower carrier frequencies, because their size in units of the wavelength is much larger.

Therefore, in this study, we present measurements of the radar cross section (RCS) of the human body in the 140-141 GHz and 219-220 GHz range. While RCS measurements for the human body have been conducted in mmWave range previously [16]–[18], to our knowledge this paper presents the first such measurements in the THz band. Furthermore, we measure *directionally resolved* RCS, i.e., for multiple angles of incidence along an arc to show how the reflectivity varies for different pairs of angles of observation.

The rest of this paper is organized as follows. The measurement equipment and experiment site are described in Section II. Section III highlights the major results for our measurement campaign. Finally, the manuscript is concluded in Section IV.

II. MEASUREMENT EQUIPMENT AND SITE

The measurements presented in the current manuscript were conducted with a custom configured frequency-domain channel sounder. In this section, we describe the testbed used

for the experimentation and provide details of the measurement site.

A. Testbed Description

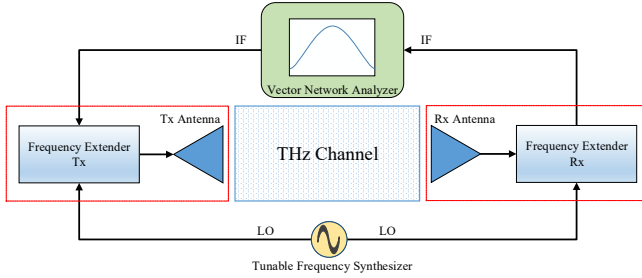


Fig. 1: VNA-based THZ measurement setup.

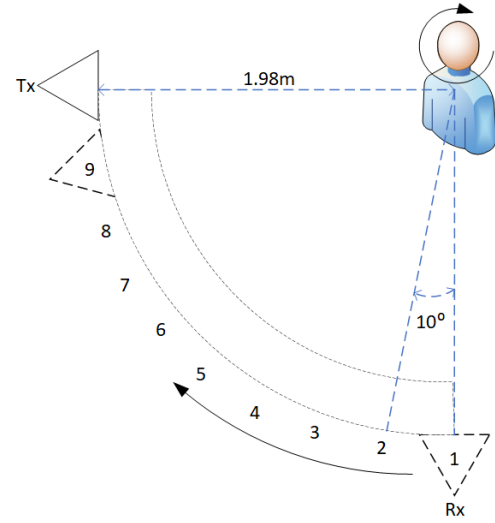
Measurement of wideband channel characteristics, which are the focus of our interest, can be conducted either by time-domain [19] or frequency-domain [12] setups. As discussed earlier, our current work is based on a frequency-domain setup. Such setups are generally known to provide excellent robustness and often act as ground truths for time-domain setups.

A diagram of our THZ equipment is shown in Fig. 1. A VNA produces Intermediate Frequency (IF) signals that are then mixed by special frequency extenders with signals from a Local Oscillator (LO) that is operating in the THz range. This THz LO signal is generated by a frequency synthesizer and it is then multiplied up into the THz range in the frequency extenders. In case the VNA has more than 2 ports, it can also produce LO signals required by the setup in Fig. 1, obviating the need for a separate frequency synthesizer. In our work, we use a 4-port VNA by Keysight Technologies (N5247A) that operates in the 0.01 - 67 GHz range to generate all the LO and the IF signals.

The frequency extenders we use are produced by Virginia Diodes Inc (VDI) that operates in the range of 140 - 220 GHz range. In order to reach the THz band, the LO signal (11.67 GHz to 18.33 GHz) is multiplied by a factor of 12. The dynamic range of these extenders is on the order of 140 dB for a special high sensitivity mode, however, for the current short distance configuration, we chose the standard sensitivity mode that has a reduced dynamic range of around 120 dB. The THz sounding signal (mixing product of IF and multiplied LO) is radiated from the transmitter (Tx) via a conical directional horn antenna with a 3dB beamwidth of 14° . The reception and downconversion at the receiver (Rx) is completely analogous. It should be noted here that the frequency extenders can have a number of different configurations and though a detailed discussion on the merits of these is beyond the scope of this paper, we make a note that our setup uses the through-reflect configuration since we are mostly interested in transmission characteristics of the channel.

B. Site Description

Fig. 2 (a) shows the site geometry of the current measurement campaign. A fixed Tx points at the torso of a mannequin



(a) Site map.



(b) Setup during measurement.

Fig. 2: Measurement site description.

that represents the human body. The Rx can move in an arc to one of 9 positions that are 10° apart thereby changing the considered angle of reflection for each case. The radius of Rx's movement arc is nearly 2m. For each Rx position, the mannequin rotates in azimuth with a step size of 20° . Tx, Rx and the mannequin's target point are all on the same height and laser crosshairs were used throughout the experiment to ensure alignment. A photograph of the setup during measurement is shown in Fig. 2 (b).

Please note that the mannequin used for these experiments does not exactly correspond to the size of an adult human, however, we conjecture that our conclusions regarding the comparisons between 140 GHz and 220 GHz band, and RCS distribution shape are independent of the mannequin size. The measurements used a mannequin instead of an actual human because it is difficult to impossible for a human to hold perfectly still (movement less than 1mm) for the duration of the VNA measurement. We furthermore note that the mannequin was dressed with a cotton T-shirt; it is known that for very short wavelengths, the properties of the clothing have more importance for the reflection properties than the dielectric properties of the body [16]. Thus, discrepancies

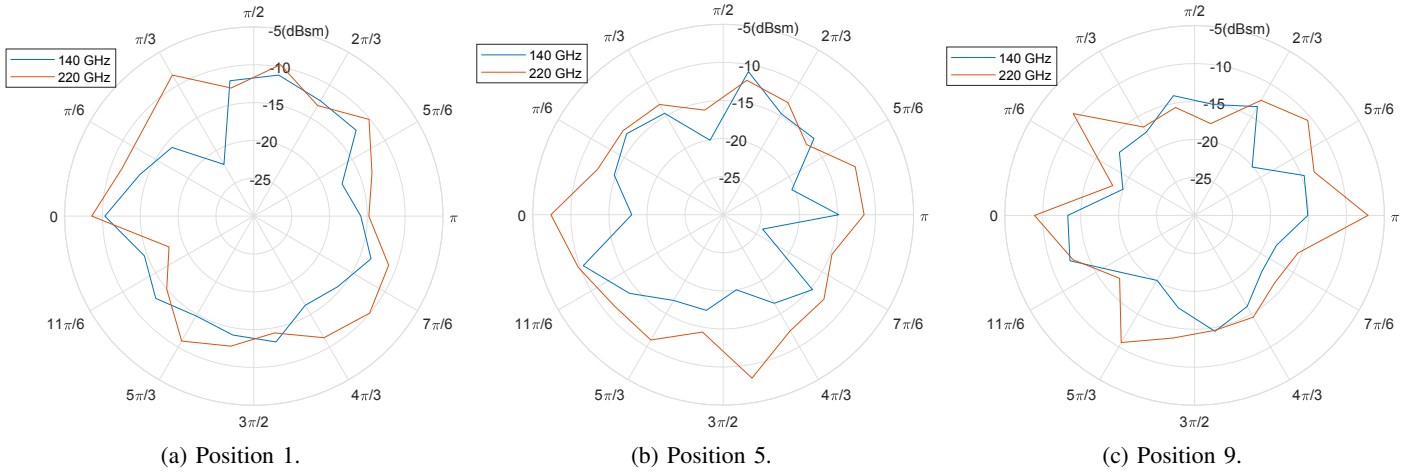


Fig. 3: Measurements of RCS for different Rx positions.

TABLE I: Setup parameters.

Parameter	Symbol	Value
Measurement points	N	201
Averaging factor	Avg	10
Bandwidth	BW	1 GHz
IF Bandwidth	IF_{BW}	500 Hz
THz IF	f_{THzIF}	279 MHz

in the characteristics between mannequin and a real human may have a minor impact on the results. Finally, we stress that different types of clothing might change the measured characteristics; such investigations are topic of ongoing work in our lab.

III. MEASUREMENT RESULTS

In this section, we present some of our key measurement methodologies and the associated results.

A. Measurement Parameters

A summary of key measurement parameters, their acronyms and nominal values is given in Table I. As discussed earlier, our frequency bands of interest include 140-141 GHz and 219-220 GHz. For each measurement, the reflections received at the Rx are delay gated to remove the contributions of reflective surfaces other than the target object. The delay gate width corresponds to reflections from within 0.5m of the target's center.

B. RCS Measurements

Using the parameters discussed in Table I, we performed a total of 18×9 measurements to cover various body orientations and Rx placements. RCS of a target object can be measured by using a standard reflector as

$$\sigma_{target} = \frac{P_{target}}{P_{std}} \frac{R_{target}}{R_{std}} \sigma_{std}, \quad (1)$$

where P_{target} is the reflected power received from the target object, P_{std} is the reflected power received by using a standard

reflector, R_{target} is the distance of the target object, R_{std} is the distance in case of the standard reflector, and σ_{std} is the calculated RCS for the standard reflector. For the current experiments, we used a metallic sphere with a radius of 0.1524m as the standard reflector. Please note that in order to keep the current study simple, we have neglected the effects of polarization on the RCS measurement and henceforth we assume that the polarization does not change with the reflection.

RCS measurements of all target orientations for three different Rx positions are shown in Fig. 3. The reflectivity seems to be in similar ranges when each of the bands under consideration is compared against itself for other Rx positions, however, we see that RCS values are higher for the 220 GHz band. These results agree with the observations of [18] that the RCS of human body increases with an increase in frequency.

The median values of RCS for all the Rx positions are shown in Fig. 4. We see a general trend that RCS decreases as the Rx position approaches the Tx position, however, there is significant scattering present on all positions. A higher RCS for the 220 GHz band is observed for the positions as well with

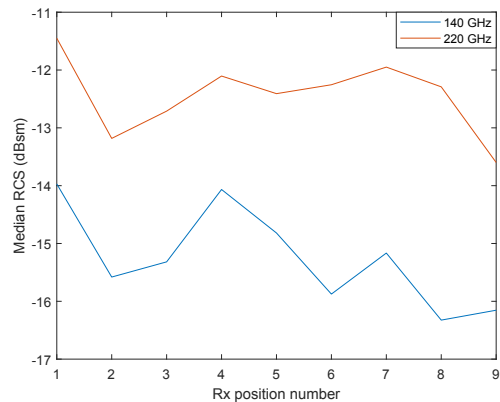
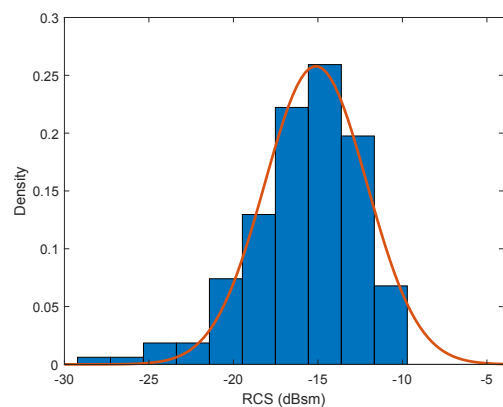
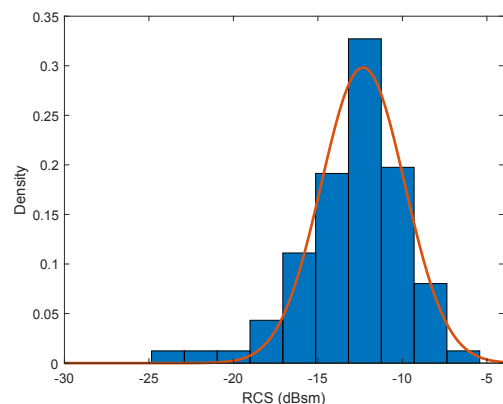


Fig. 4: Median RCS for different Rx positions.



(a) 140 GHz.



(b) 220 GHz.

Fig. 5: Histogram of RCS values for all positions.

a nearly -2 dBsm difference between both the two cases. The values we measured in the current experiments are less than -11.1 dBsm reported for 79 GHz measurements presented in [17], however, it should be noted there is a difference between the target size for both the studies.

The histograms and distributions of measurements in both the frequency bands are shown in Fig. 5. In both cases, we found that a normal distribution provides the best fit as opposed to Weibull or Log-normal distribution suggested by other studies such as [17], [18].

IV. CONCLUSION

THz communication has evoked a deeper interest in recent years. However, before an eventual deployment can be undertaken, detailed channel measurements are required for the characterization of key deployment scenarios. Since humans are present in all these environments, it is important to know the impact our bodies cause on the propagation of these high frequency channels. In this regard, we conducted measurements of radar cross section (RCS) for the human body at 140 and 220 GHz bands. Our results show that RCS values increase with frequency, and that they are distributed according to a normal distribution. In our future work, we plan to investigate

further typical indoor and outdoor communication scenarios and their key components.

REFERENCES

- [1] K.-C. Huang and Z. Wang, "Terahertz Terabit Wireless Communication," *Microwave Magazine, IEEE*, vol. 12, no. 4, pp. 108–116, June 2011.
- [2] M. Shafi, A. F. Molisch, P. J. Smith, T. Haustein, P. Zhu, P. D. Silva, F. Tufvesson, A. Benjebbour, and G. Wunder, "5G: A Tutorial Overview of Standards, Trials, Challenges, Deployment and Practice," *IEEE Journal on Selected Areas in Communications*, 2017.
- [3] A. Hirata and M. Yaita, "Ultrafast Terahertz Wireless Communications Technologies," *IEEE Transactions on Terahertz Science and Technology*, vol. 5, no. 6, pp. 1128–1132, Nov 2015.
- [4] I. F. Akyildiz, J. M. Jornet, and C. Han, "TeraNets: ultra-broadband communication networks in the terahertz band," *IEEE Wireless Communications*, vol. 21, no. 4, pp. 130–135, August 2014.
- [5] H. J. Song and T. Nagatsuma, "Present and Future of Terahertz Communications," *IEEE Transactions on Terahertz Science and Technology*, vol. 1, no. 1, pp. 256–263, Sept 2011.
- [6] T. Kürner and S. Priebe, "Towards THz Communications - Status in Research, Standardization and Regulation," *Journal of Infrared, Millimeter, and Terahertz Waves*, vol. 35, no. 1, pp. 53–62, 2014.
- [7] I. F. Akyildiz, J. M. Jornet, and C. Han, "Terahertz band: Next frontier for wireless communications," *Physical Communication*, vol. 12, pp. 16 – 32, 2014.
- [8] N. Khalid, N. A. Abbasi, and O. B. Akan, "Capacity and coverage analysis for fd-mimo based thz band 5g indoor internet of things," in *Personal, Indoor, and Mobile Radio Communications (PIMRC), 2017 IEEE 28th Annual International Symposium on*. IEEE, 2017, pp. 1–7.
- [9] FCC, "Fcc takes steps to open spectrum horizons for new services and technologies," <http://docs.fcc.gov/public/attachments/DOC-356588A1.pdf>, 2019.
- [10] Y. Kim, H. Ji, J. Lee, Y.-H. Nam, B. L. Ng, I. Tzanidis, Y. Li, and J. Zhang, "Full dimension mimo (fd-mimo): The next evolution of mimo in lte systems," *IEEE Wireless Communications*, vol. 21, no. 2, pp. 26–33, 2014.
- [11] M. Y.-W. Chia, B. Luo, and C. K. Ang, "Extremely wideband multipath propagation channel from 285 to 325 ghz for a typical desk-top environment," in *Infrared Millimeter and Terahertz Waves (IRMMW-THz), 2010 35th International Conference on*. IEEE, 2010, pp. 1–1.
- [12] S. Priebe, C. Jastrow, M. Jacob, T. Kleine-Ostmann, T. Schrader, and T. Kürner, "Channel and propagation measurements at 300 GHz," *Antennas and Propagation, IEEE Transactions on*, vol. 59, no. 5, pp. 1688–1698, 2011.
- [13] S. Kim and A. G. Zajić, "Statistical characterization of 300-ghz propagation on a desktop," *IEEE Transactions on Vehicular Technology*, vol. 64, no. 8, pp. 3330–3338, 2015.
- [14] N. Khalid, N. A. Abbasi, and O. B. Akan, "Statistical characterization and analysis of low-thz communication channel for 5g internet of things," *Nano Communication Networks*, vol. 22, p. 100258, 2019.
- [15] N. A. Abbasi, A. Hariharan, A. M. Nair, A. S. Almainan, F. B. Rotenberg, A. E. Willner, and A. F. Molisch, "Double directional channel measurements for thz communications in an urban environment," *arXiv preprint arXiv:1910.01381*, 2019.
- [16] N. Yamada, Y. Tanaka, and K. Nishikawa, "Radar cross section for pedestrian in 76ghz band," in *2005 European Microwave Conference*, vol. 2. IEEE, 2005, pp. 4–pp.
- [17] M. Yasugi, Y. Cao, K. Kobayashi, T. Morita, T. Kishigami, and Y. Nakagawa, "79ghz-band radar cross section measurement for pedestrian detection," in *2013 Asia-Pacific Microwave Conference Proceedings (APMC)*. IEEE, 2013, pp. 576–578.
- [18] T. Motomura, K. Uchiyama, and A. Kajiwara, "Measurement results of vehicular rcs characteristics for 79ghz millimeter band," in *2018 IEEE Topical Conference on Wireless Sensors and Sensor Networks (WiSNet)*. IEEE, 2018, pp. 103–106.
- [19] Y. Xing and T. S. Rappaport, "Propagation measurement system and approach at 140 ghz-moving to 6g and above 100 ghz," in *2018 IEEE Global Communications Conference (GLOBECOM)*. IEEE, 2018, pp. 1–6.